Numerical analysis of the hydrogen-air mixture formation process in a direct-injection engine for off-road applications

International Journal of Hydrogen Energy 77 (2024) 1286–1295

Contents lists available at ScienceDirect

International Journal of Hydrogen Energy

journal homepage: www.elsevier.com/locate/he

Numerical analysis of the hydrogen-air mixture formation process in a direct-injection engine for off-road applications

A. Scalambro [a], A. Piano [a,*], F. Millo [a], N. Scinicariello [b], W. Lodi [b], A. Dhongde [c], G. Sammito [d]

[a] Politecnico di Torino, Torino, Italy
[b] Kohler Energy, Reggio Emilia, Italy
[c] FEV Europe GmbH, Aachen, Germany
[d] FEV Italy, Torino, Italy

ARTICLE INFO

Handling Editor: Dr M Mahdi Najafpour

Keywords:
Hydrogen engine
Alternative fuels
3D-CFD
Hydrogen direct-injection
Mixture homogeneity
Retrofitability

ABSTRACT

Among the different hydrogen premixed combustion concepts, direct injection (DI) is one of the most promising for internal combustion engine (ICE) applications. However, to fully exploit the benefits of this solution, the optimization of the mixture preparation process is a crucial factor. In the present work, a study of the hydrogen-air mixture formation process in a DI H_2-ICE for off-road applications was performed through 3D-CFD simulations. First, a sensitivity analysis on the injection timing was carried out to select the optimal injection operating window, capable of maximizing mixture homogeneity, without a significant volumetric efficiency reduction. Then, different spray injector guiding caps were tested to assess their effect on in-cylinder dynamics and mixture characteristics consequently. Finally, the impact of swirl intensity on hydrogen distribution has been assessed. The optimization of the combustion chamber geometry has allowed the achievement of significant improvements in terms of mixture homogeneity.

1. Introduction

Despite attempts to reduce greenhouse gas emissions, carbon dioxide (CO2) emissions resulting from human activities have steadily risen in recent decades [1]. This has led to an escalation in global temperatures and the onset of climate change, further emphasizing the urgent need to move toward a climate-neutral economy [2]. Among all the energetic sectors, the transportation sector represents one of the most important contributors to this upward trend, accounting for around 25% of the total global CO2 emissions [3]. Moreover, emissions linked to transportation grew faster than any other sector exhibiting an annual average rate of 1.7% from 1990 to 2022. Due to this, governments are fostering stringent measures to reduce the environmental footprint of this sector [4]. For this purpose, the European Union (EU) has targeted a 55% reduction in CO2 emissions by 2030, as outlined in the Fit for 55 packages [5], in line with the challenging objective of achieving climate neutrality for Europe by 2050 as part of the European Green Deal [6].

In this framework, hydrogen is expected to play a key role in the transition toward a climate-neutral economy thanks to its excellent capacity for seamless integration with renewable energy sources. As a matter of fact, it can be produced from renewable energy sources and integrated into the existing transportation infrastructure. Additionally, it is both an energy carrier and energy vector, effectively mitigating challenges associated with the intermittency of renewable energy sources and their uneven geographical distribution. Among the different solutions currently under development, the use of hydrogen as a fuel for internal combustion engines represents one of the most promising, thanks to their relatively high efficiency, especially at high loads [7]. Moreover, H_2-ICE can exploit the maturity of the manufacturing processes and facilities [8] along with easier integration within the currently available powertrains. Additionally, in comparison to conventional fossil fuels, hydrogen features excellent combustion properties [9,10], such as a high lower heating value (LHV), (i.e. 120 MJ/kg) [8], a fast flame propagation over a wide range of thermo-chemical conditions [11,12], a high lean-burn limit, and a high knock resistance [13,14], making it particularly suitable for being used as a fuel in internal combustion engines. Nonetheless, the low volumetric density of hydrogen [10] leads to a theoretical reduction of the power output of about 15% compared to a gasoline engine [15]. Moreover, the need to work at high relative air-to-fuel ratios to reduce combustion temperatures, NOx emissions [16] and avoid abnormal combustion might further increase the power deficit of the engine by up to 30%. Direct Injection (DI)

* Corresponding author.
E-mail address: andrea.piano@polito.it (A. Piano).

https://doi.org/10.1016/j.ijhydene.2024.06.193
Received 6 May 2024; Received in revised form 10 June 2024; Accepted 13 June 2024
Available online 22 June 2024

represents an effective solution to compensate for the above-mentioned detrimental phenomena. Indeed, for the same operating relative air-to-fuel ratio, the exploitation of a DI technology avoids the reduction of volumetric efficiency and the consequent performance losses, thus allowing the simplification of the design of the charging system at the same time. Moreover, the injection of hydrogen directly inside the combustion chamber significantly reduces the risk of abnormal combustion phenomena such as backfiring [17]. Finally, DI leads also to the reduction of the compression work further increasing the overall efficiency. However, this solution gives rise to some challenges that have to be tackled to fully exploit its benefits, mainly related to the mixture preparation process. Indeed, hydrogen combustion in DI engines may enhances particles formation [18]. Nevertheless, particle formation can be limited by properly tuning injection pressure and timing [19]. Additionally, the achievement of a sufficiently homogeneous mixture is of paramount importance to limit NOx emissions [20] and ensure a stable combustion. Compared to other gaseous fuels, such as natural gas, hydrogen is characterized by a higher diffusivity [21]. Nonetheless, the long injection duration linked to its low density and the short time available for air-hydrogen mixing severely hinder a balanced hydrogen distribution within the combustion chamber. This issue might be mitigated to some extent by advancing the injection process. Despite this, too early injection timings might reduce the volumetric efficiency [22], and increase the compression work, partially jeopardizing the benefits induced by a DI concept. Alternatively, higher injection pressures can be exploited to reduce the injection duration and promote the hydrogen-air mixing. Nonetheless, the implementation of high-pressure injectors would lead either to the reduction of the vehicle range or the necessity of implementing an H_2 re-compression system to maximize the use of stored fuel, thus increasing the degree of complexity [23]. For all these reasons, most of the OEMs are currently focusing their efforts on the development of H2-ICEs equipped with a low-medium pressure DI system, representing the best trade-off between performance and complexity.

In this context, 3D-CFD simulations based on Reynolds Averaged Navier-Stokes (RANS) approach represent a valuable tool to optimize the injection and mixture formation processes, thus significantly supporting the engine design process, reducing the time-to-market, thus breaking down development costs. Indeed, numerical simulations can provide additional details concerning the mixture formation process which cannot be directly gathered from experimental campaigns. In turn, these data can be exploited to obtain a deeper understanding of the main factors that contribute to or hinder a homogeneous distribution of hydrogen in the combustion chamber. Li et al. [24] performed a numerical study to find the injection timing capable of maximizing the thermal efficiency and the formation process of the hydrogen-air mixture of a DI hydrogen engine: for highly advanced injection timing, the additional work needed to compress the hydrogen reduces the indicated thermal efficiency, while for excessively late injections the reduction of mixture uniformity significantly increases NOx emissions. However, only the injection timing, strategy (e.g. single injection and multiple injection), and the injection pressure were varied, while little attention was given to the geometry of the combustion chamber. Similarly, Hamzehloo et al. [25] analyzed the mixture formation process under different injection strategies (i.e., single injection and double injection) in a pent-roof engine. They found that a double injection strategy can increase uniformity and strengthen the turbulent flow field at the same time. In Ref. [26] the effect of the start of injection on a single cylinder spark ignition engine was investigated for different relative air-to-fuel ratios. It turned out that the start of injection has a significant impact on mixture properties and on combustion process for relative air-to-fuel ratios greater than 3. However, this analysis was carried out at low engine speed (1000 rpm), thus significantly increasing the mixing time. The impact that different injector funnel geometries can have on the properties of the mixture was assessed in a hydrogen engine retrofitted from a high-performance turbocharged gasoline engine, by Durand et al. [27]. Nevertheless, the selected case study was originally designed for achieving high tumble intensities, thus increasing turbulence intensity during compression, generally resulting in improved mixing. On the contrary, there is still very little scientific understanding of the optimization of a combustion chamber retrofitted from a diesel engine, and there are no studies in the literature that address the topic systematically. In light of this, the goal of this study is the optimization of the mixture properties of a relatively small displacement (~0.6 l/cyl.) DI H_2-ICE for off-road applications retrofitted from a diesel engine. To the best of the author's knowledge, most of the H_2-ICEs currently under development are quite large engines for heavy-duty applications [28], since electrification is usually preferred for small engines [29]. But when dealing with off-road applications there are several aspects such as the maximization of the machine productivity, the reduction of the refueling-recharging time, the minimization of the operative cost, and the need for operational flexibility that, make this solution particularly attractive when considered all together.

The conversion of a diesel engine for being used with hydrogen in a direct injection configuration requires several software and hardware changes. For what concerns the latter in addition to the reduction of the compression ratio, and the adaptation of the turbocharging system, the integration of the injection and ignition systems into the cylinder head may require significant modifications to the combustion system. In order to reduce the conversion costs and to assess the retrofit ability of a diesel engine for being operated with hydrogen in a DI configuration, only minor geometrical modifications were introduced to the original combustion system. Specifically, the paper is organized as follows: first, the case study is presented, along with the set-up of the 3D-CFD model used to carry out the simulation activity. Then, the effects of the injection timing on in-cylinder dynamics and the filling process will be shown. After having identified the optimal injection timing, the paper focuses on the sensitivity to the geometry of the spray cap, highlighting the impact of different spray cap geometries on the main motion patterns and mixture homogeneity. Finally, a sensitivity on the eccentricity of the intake valve seats is reported to assess the effect of swirl on the hydrogen-air mixing process. The modifications introduced to the operational and geometrical parameters of the combustion chamber allowed to achieve a significant improvement in terms of hydrogen distribution.

2. Case study

A four-cylinder diesel engine equipped with a high-pressure common rail injection system was selected as a case study. It features a unitary displacement of 0.62 l with a fixed valve actuation, achieving a maximum power of 55 kW at 2600 rpm and a maximum torque of 315 Nm at 1500 rpm. To keep as low as possible the conversion costs, the main geometrical characteristics of the engine were not altered in the conversion process (Table 1). Therefore, the same displacement, bore and stroke of the original diesel engine were adopted, and both the cylinder head and the intake and exhaust ports have not been subject to any change. Nonetheless, a reduction of the compression ratio (CR) from 17:1 to 11:1 has been required to guarantee a stable and knock-free combustion at high loads. To this end, the piston bowl reported in Fig. 1 was exploited to increase the clearance volume, thus allowing the CR reduction. Moreover, this shape of the piston bowl was also partially

Table 1
Main specifications of the SI H_2-DI ICE.

Displacement [l/cyl.]	0.62
Bore [mm]	88
Stroke [mm]	102
Compression Ratio [−]	11
Number of cylinders [−]	4
Rated Power [kW]	55 @ 2600 rpm
Max. Torque [Nm]	315 @ 1500 rpm

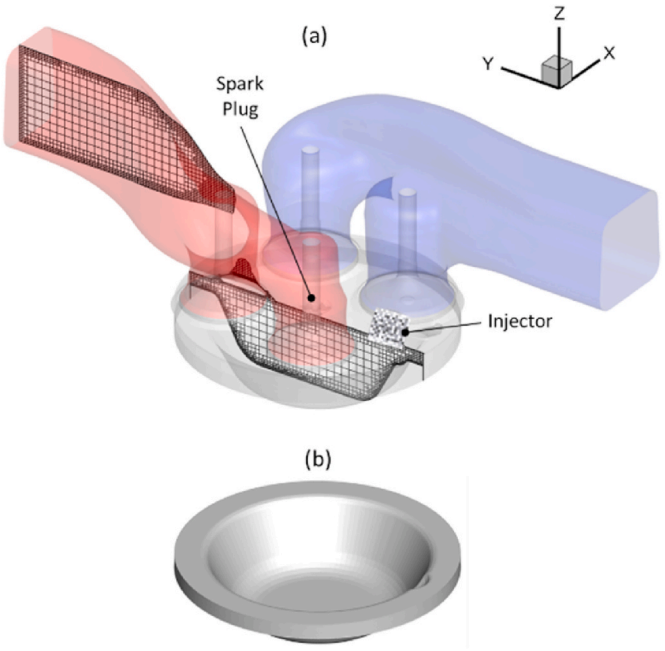

Fig. 1. Fluid domain 20 CAD before TDC firing, with a cross-section passing through the injector axis (a), and piston geometry (b).

constrained by cooling requirements, further reducing the number of degrees of freedom to act upon. The spark plug was integrated into the cylinder head replacing the original diesel injector. An outwardly opening hydrogen injector specifically designed for direct injection operations, featuring a maximum injection pressure of 30 bar was positioned laterally, close to the cylinder liner on a plane between the intake and exhaust ports. The implementation of the injection system in a central position has been impeded by the reduced space available among the four valves, which would have led to an excessively small metal bridge, with reduced mechanical resistance and poor heat dissipation properties.

Simulations were performed in the rated power working point (2600 rpm $\times$ 10.3 bar) since the combination of the large amount of injected hydrogen with the relatively high engine speed, makes this operating condition one of the most challenging for obtaining a satisfactory mixture homogeneity. In this operating condition, a target relative air-to-fuel ratio equal to 2.3 was selected since NOx production should be almost nil if a perfectly homogeneous mixture is achieved [16], thus avoiding the need to install dedicated after-treatment systems. Each component of the system has been designed to achieve the same performance (in terms of full load curve) as the original diesel engine.

3. Numerical model

Simulations were performed by means of the commercially available software Converge 3.0.25. The description of the turbulent flow field is of paramount importance for an accurate description of the injection and the hydrogen-air mixing processes. Even though Large Eddy Simulations (LES) can provide a deeper level of understanding of these phenomena, the increase in the computational efforts induced by the need to adopt an extremely fine mesh and the consequent reduction of the simulation time-step, make this choice unfeasible and not compatible with the temporal constraints of industrial development. Therefore, a RANS approach, coupled with the $k-\varepsilon$ with the renormalization group (RNG) turbulence model was adopted. Negligible differences arise from the adoption of one of the $k-\varepsilon$ turbulence models (i.e. $k-\varepsilon$ *standard*, $k-\varepsilon$ *RNG* and $k-\varepsilon$ *realizable*) [30]. Nonetheless, the *RNG* $k-\varepsilon$ model was chosen since it is especially well-suited for capturing the evolution of strongly rotating vortices, such as swirl and tumble, thereby enhancing the prediction accuracy [31] of the simulation. Time-varying boundary conditions in terms of pressure and temperature, and wall temperatures were adopted from a 1D-CFD complete engine model, developed in GT-SUITE v2023. The injection event was modeled by imposing both the injection pressure and the injector valve motion profile, thus giving hydrogen mass flow rate as a simulation output. This latter was then compared with the experimental measurements for validation purposes. The fluid domain was discretized through an orthogonal mesh, as reported in Fig. 1, with a base grid size of 2.8 mm, and local mesh refinements were added in the volume close to the valve face, to properly characterize the gas exchange process. Moreover, the Adaptive Mesh Refinement (AMR) algorithm was exploited to automatically refine the mesh, achieving a minimum grid size of 0.35 mm. Additionally, an extremely small grid size (0.0875 mm) was included within the injector nozzle. Finally, the computational domain in the neighboring of the boundaries of the combustion chamber was permanently refined since its resolution has shown a significant impact on hydrogen diffusion [32]. The time step was controlled employing a variable time step algorithm. More in detail it was constrained by the maximum Courant Friedrich Lewy (CFL) numbers, whose values were chosen in agreement with those generally found in the literature ($CFL_{Convection} = 1.0$, $CFL_{Diffusion} = 2.0$, $CFL_{Mach} = 50.0$) [33]. The adoption of such a refined mesh with the above-mentioned CFL numbers reduced the time step down to 10^{-8} s during the injection. The kinetic and thermal boundary layers were modeled adopting the law of the walls functions. Finally, heat transfer was described by means of the O'Rourke and Amsden model [34], as it was successfully exploited for conventional spark ignition engines [35,36], pre-chamber equipped engines [37] and non-premixed concepts (e.g. compression-ignition engines) [38]. The numerical model has been validated against experimental data gathered from a chamber with optical access for a wide range of injection pressure, ambient pressure and injection duration [39].

4. Simulation results

4.1. Effects of injection timing

At first, a sweep of injection timings was conducted with the goal of identifying the optimal injection timing that could maximize mixture uniformity without significantly affecting volumetric efficiency and preventing hydrogen backflow into the intake ports. Three start of injection (SOI) timings were considered in the analysis. The starting SOI was set at 180 CAD bTDCf to phase the entire injection event after the intake valve closing (IVC). This is the most conservative condition since hydrogen backflow is a priori avoided and the reduction of volumetric efficiency induced by the partial replacement of the inflow air by the expansion of the hydrogen is prevented. Afterward, SOI was advanced by 30 CAD (i.e. 210 CAD bTDCf) and 60 CAD (i.e. 240 CAD bTDCf) compared to the base timing. Lastly, injection duration was kept constant for the tested SOIs.

As reported in Fig. 2, the helical shape of the intake ports generates a quite intense swirl motion, whereas the tumble ratio both on the ZX (hereafter referred to as Y-tumble) and ZY (hereafter referred to as X-tumble) planes is almost nil at the intake valve closing (IVC). The injection process has a negligible impact on the evolution of the swirl (Fig. 2a). Indeed, the swirl ratio is reduced by less than 10% compared to the swirl ratio resulting from an engine cycle without injection. This is mainly due to the orientation of the injector axis, since being almost vertical and parallel to the cylinder axis intrinsically reduces the interaction between the hydrogen jet and any organized structured motion pattern that rotates about the cylinder axis. Instead, the entrance of a high-speed jet within the combustion chamber leads to an important growth of both the X-tumble and Y-tumble ratios thanks to the interaction between the hydrogen jet and the boundaries of the combustion

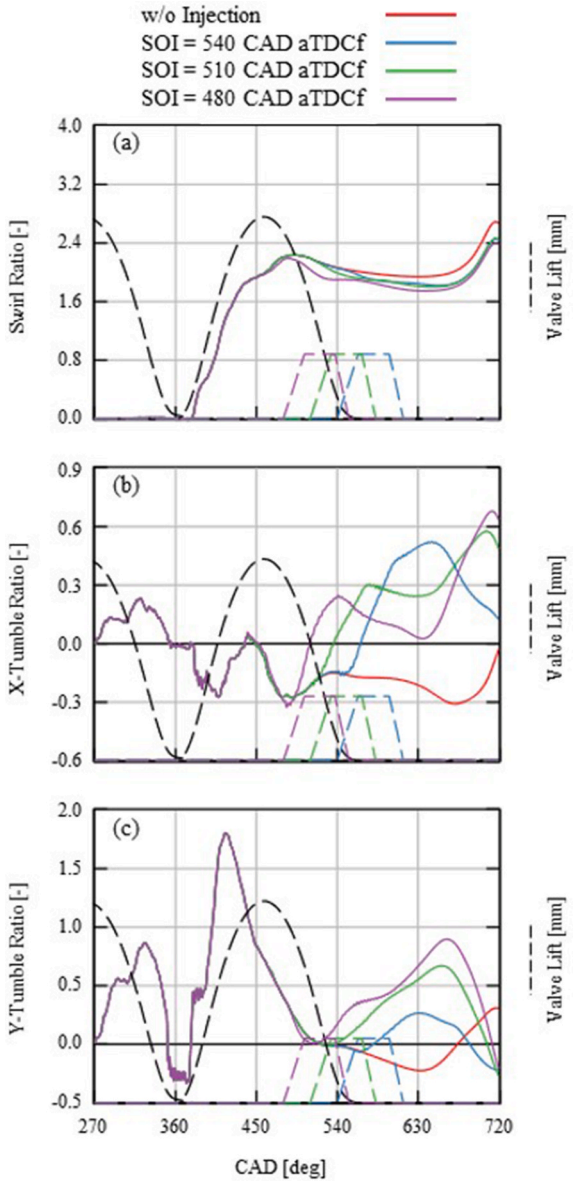

Fig. 2. Swirl Ratio (a), X-Tumble Ratio (b), and Y-Tumble Ratio (c) for an engine cycle without injection, and three engine cycles with the start of injection at 180 CAD, 210 CAD, and 240 CAD before TDC firing.

chamber. As reported in Fig. 2b and c, tumble intensity varies with the injection timing because of the different positions occupied by the piston when is wetted by the incoming hydrogen. More in detail, the X-tumble ratio decreases during the injection process while it is enhanced close to the TDCf for more advanced SOI. Y-tumble monotonically increases advancing the injection.

In Fig. 3a and b, the total in-cylinder mass and the mass of hydrogen into the intake ports are reported considering the three injection timings previously mentioned. As already mentioned, the phasing of the injection event after the IVC does not reduce volumetric efficiency and inherently avoids possible hydrogen slips into the intake ports. When the SOI is advanced at 210 CAD bTDCf, the gaseous injection pushes back into the intake ports part of the in-cylinder air, resulting in a 2% reduction of volumetric efficiency. Nevertheless, a negligible amount of hydrogen is noticed in the intake runners thanks to the almost vertical entrance of the injected gas that moves away hydrogen from the intake valves during the last phase of the intake stroke. On the contrary, a further SOI advance heavily reduces volumetric efficiency by about 10%

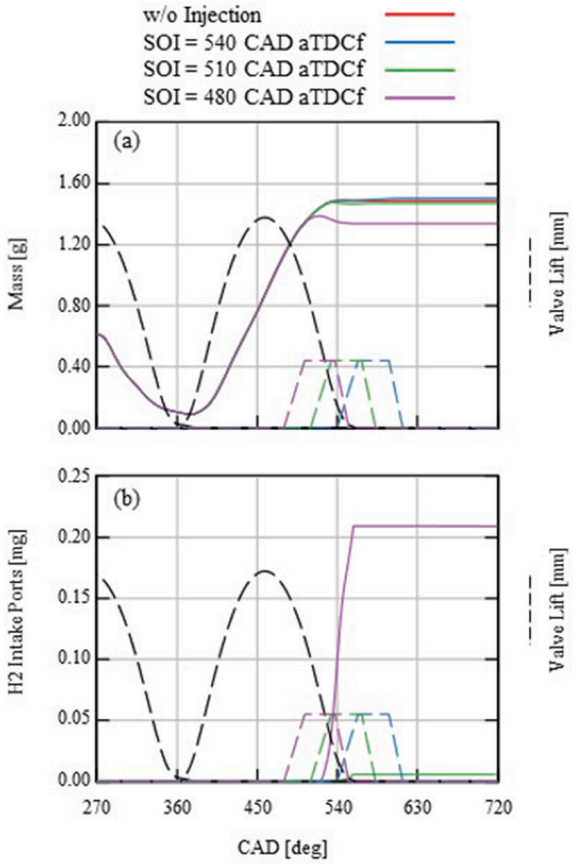

Fig. 3. In-cylinder total mass (a), and hydrogen mass in the intake ports (b) for an engine cycle without injection, and three engine cycles with the start of injection at 180 CAD, 210 CAD, and 240 CAD before TDC firing.

compared to the engine cycle without injection, and a significant mass of hydrogen moves into the intake ports.

Fig. 4 shows lambda distribution on three different sections at 20 CAD bTDCf for the three injection timings analyzed so far. With the most delayed SOI (180 CAD bTDCf - Fig. 4a), the uniformity level of hydrogen is fairly low. Indeed, an extremely lean region ($\lambda > 5$) is present on the opposite side of the H_2-injector while an almost stoichiometric mixture is obtained close to the liner in correspondence with the intake valves. To numerically quantify the degree of mixture homogeneity, the relative equivalence ratio parameter (Φ_{Rel}) was exploited. It is computed as the ratio between the standard deviation of the equivalence ratio and the average value of the equivalence ratio.

$$\Phi_{Rel} = \frac{\sigma_{\Phi}}{\Phi_{AVG}} \tag{1}$$

Thereby, extremely uniform mixtures are characterized by relatively low Φ_{Rel} ($\Phi_{Rel} < 25\%$), while particularly uneven mixtures will show higher Φ_{Rel} values. When advancing the SOI from 180 to 210 CAD bTDCf (Fig. 4b), mixture homogeneity significantly increases, as confirmed by the reduction of Φ_{Rel} (−15% absolute). As a matter of fact, the advance in injection timing increases the time that hydrogen has available for spreading into the combustion chamber. Due to this, the stoichiometric region observed with the most delayed SOI is no longer present and the volume occupied by the previously noticed lean mixture is significantly reduced. Nonetheless, a vertical stratification of the mixture can be noticed, with a higher fuel concentration close to the piston top and a higher λ closer to the spark plug, which might affect combustion variability. This issue is partially improved for SOI = 240 CAD bTDCf, since a mixture with $\lambda \sim 2$ is achieved in the neighboroods of the spark plug. However, a minor improvement in terms of Φ_{Rel} is obtained compared to

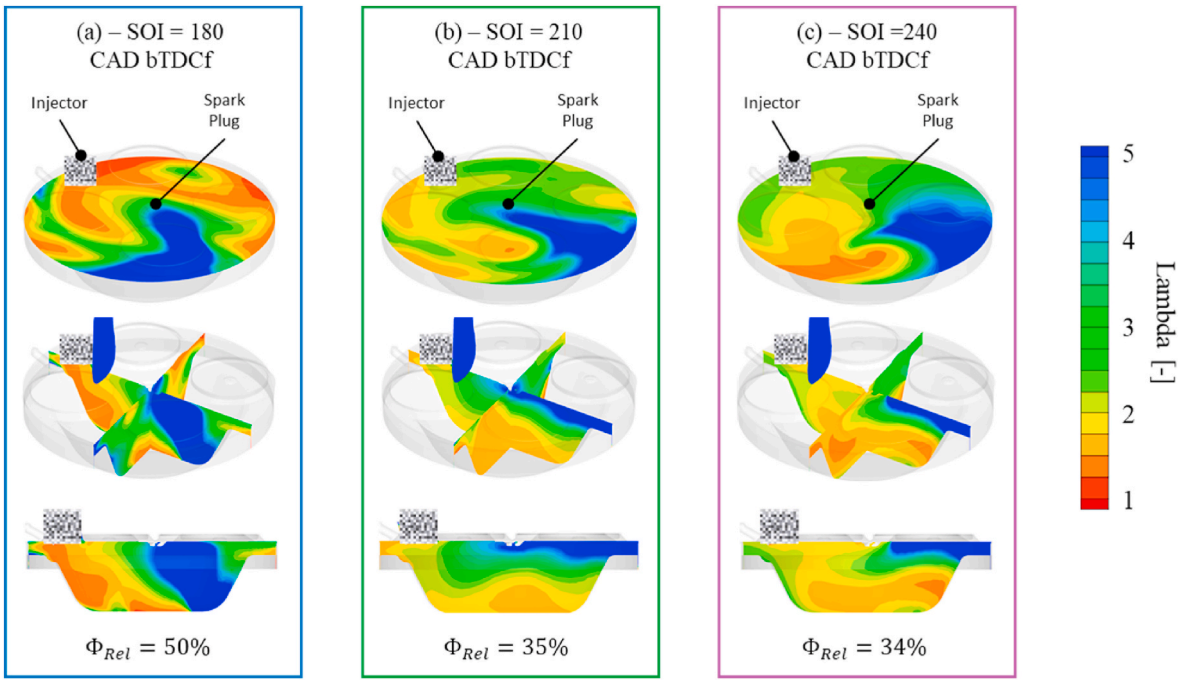

Fig. 4. Lambda distribution 20 CAD before TDC firing for the start of injection at 180 CAD (a), 210 CAD (b), and 240 CAD (c) before TDC firing.

that achieved advancing the SOI from 180 to 210 CAD bTDCf. Moreover, mixture properties remain overall quite similar to those achieved with more delayed SOI, since hydrogen spreads more difficulty on the opposite side of the injector, while its concentration is higher close to the injector, near the liner and the piston. This suggests that, even if injection timing plays a crucial role in determining mixture properties, there are some limits strictly related to the features of the combustion system and specifically to the in-cylinder dynamics that hinder the mixture uniformity level.

In Fig. 5 the volumetric efficiency reduction compared to the engine cycle without injection and the Φ_{Rel} are displayed as a function of the injection timing. As previously shown in Fig. 3a, filling losses are nil when the injection entirely occurs after the IVC, while they are about 2% and 10% for SOI = 210 CAD and SOI = 240 CAD bTDCf respectively. On the other side, a considerable uniformity improvement is achieved by advancing the SOI from 180 CAD to 210 CAD bTDCf, whereas mixture homogeneity does not improve for SOI = 240 CAD bTDCf. Hence, SOI = 210 CAD was selected as the optimal injection timing since it improves mixture properties without severely affecting the cylinder filling process, thus avoiding engine operations with lower relative air-to-fuel ratios. Because of these reasons, this injection timing has been considered for the continuation of the analysis.

4.2. *Effects of spray cap design*

In-cylinder dynamics have a central role in determining combustion characteristics since they heavily affect the evolution of the hydrogen plume. However, the high speed of hydrogen flow that enters the combustion chamber impacts the cylinder motion patterns. Accordingly, the injection process can be exploited to obtain suitable dynamics. More in detail the interaction between the hydrogen plume and the combustion chamber walls can be modified by acting on the design of the injector spray cap, which can be used to provide a preferential direction

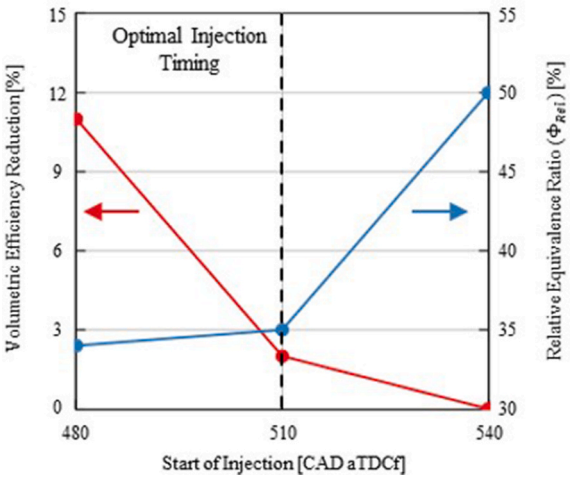

Fig. 5. Reduction of the Volumetric Efficiency and Relative Equivalence Ratio as a function of the Start of Injection.

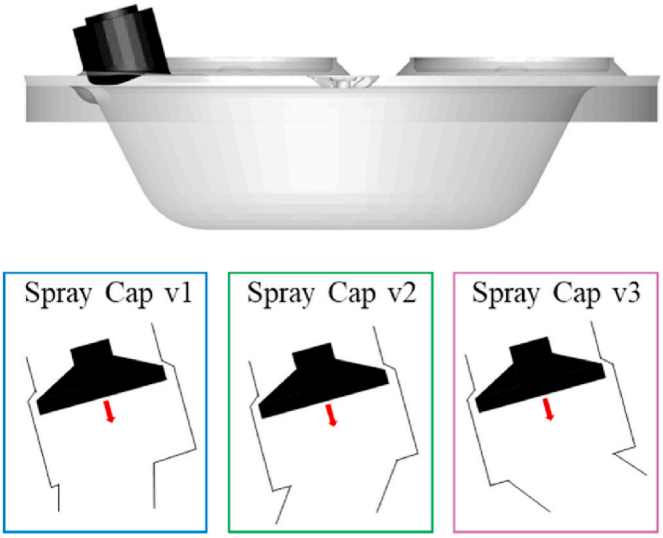

Fig. 6. Spray Guiding Cap geometries.

to the hydrogen jet.

In Fig. 6 the schematics of three spray guiding caps are reported. Results shown in paragraph 4.1 were achieved by adopting the cap here referred to as *Spray Cap v1*. It is a single-nozzle cap with a vertical hole drilled on the liner side of the cap. This specific design was defined with the aim of obtaining a vertical entrance of the hydrogen jet and exploiting the upward movement of the piston to convert the injection energy into a structured rotation pattern (X-Tumble). A second spray cap (*Spray Cap v2*) was designed with the same purpose. It features a single nozzle drilled into the center of the guiding cap but tilted toward the cylinder liner. Lastly, *Spray Cap v2* has been rotated 180° about the injector axis (*Spray Cap v3*). This spray cap has been tested to assess the homogeneity benefits that can be achieved by injecting hydrogen toward a wider fresh charge volume. For all the above-mentioned spray cap designs, the same injection strategy, in terms of injection timing (SOI = 210 CAD bTDCf) and injection pressure (p_{inj} = 25 *bar*) was adopted.

As already mentioned, the impact of the injection event on the swirl intensity is intrinsically reduced by the vertical orientation of the injector. Therefore, the adoption of different spray guiding caps does not modify swirl evolution, as displayed in Fig. 7a. On the other hand, sensible differences can be noticed in the evolution of the tumble (Fig. 7b and c) changing the cap. Indeed, while *Spray Cap v1* leads to fairly moderate X-tumble and Y-tumble ratios, both *Spray Cap v2* and *Spray Cap v3* lead to a noticeable X-tumble increase, due to the more tilted hydrogen spray axis.

The reasons for this behavior can be understood by looking at Fig. 8, where an iso-surface with a hydrogen concentration of 1% is reported at 180, 135, and 100 CAD bTDCf to identify the external periphery of the hydrogen plume. Adopting *Spray Cap* v1 (Fig. 8a), hydrogen is split into two main paths before the end of injection (i.e. 180 CAD bTDCf). One of them moves toward the center of the combustion chamber and the other one runs vertically, remaining attached to the cylinder liner. This division remains quite clear even after the end of the injection (i.e. 135 CAD bTDCf). Because of this, the interaction between the injected hydrogen and the bowl of the piston is quite limited and the bulk air flow motion is overall balanced. Therefore, during the compression stroke (i.e. 100 CAD bTDCf) swirl represents the most predominant motion as previously shown in Fig. 7. Instead, *Spray Cap v2* (Fig. 8b) is very effective in directing all the injected hydrogen vertically toward the bowl of the piston. When the hydrogen impinges on the side of the piston bowl, it is

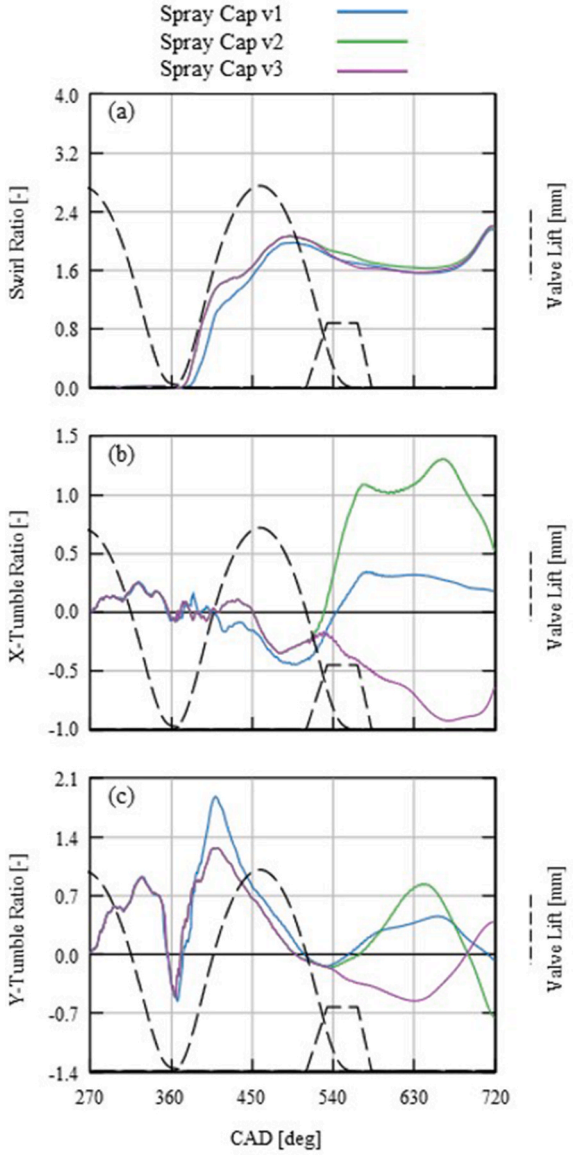

Fig. 7. Swirl Ratio (a), X-Tumble Ratio (b), and Y-Tumble Ratio (c) for Spray Cap v1, Spray Cap v2 and Spray Cap v3.

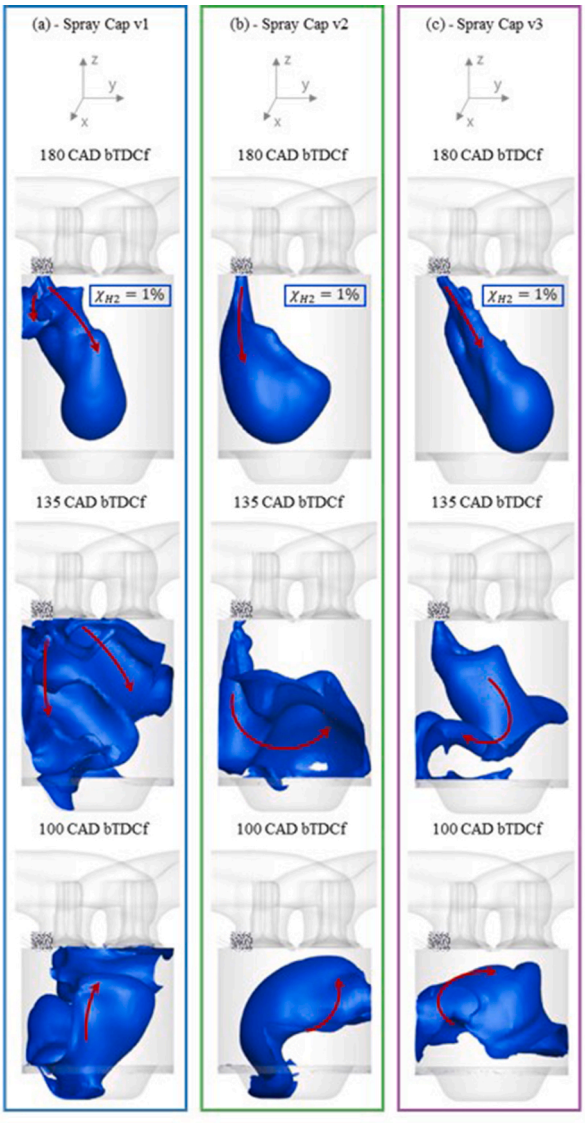

Fig. 8. Hydrogen morphology at 180 CAD, 585 CAD, and 620 CAD for Spray Cap v1 (a), Spray Cap v2 (b), and Spray Cap v3 (c).

deflected, contributing to the generation of a strong tumble motion that rotates on a plane normal to the YZ plane (X-tumble). Thanks to this, the injected hydrogen can effectively reach the side of the cylinder opposite to the injector. Moreover, the tumble motion induces a folding motion to the mixture, which in turn should help in increasing mixture homogeneity. As expected, *Spray Cap v3* (Fig. 8c) is very effective in directing the injected hydrogen since it is directly derived from *Spray Cap v2*. Adopting this cap, hydrogen is injected toward the center of the combustion chamber. Hence, in contrast to the observations made with *Spray Cap v2*, the hydrogen jet impacts the opposite side of the piston bowl, generating a tumble motion with a reversed rotation direction.

In Fig. 9, the hydrogen distributions achieved with the above-mentioned spray caps are reported 20 CAD bTDCf. Among them, *Spray Cap v1* leads to the most homogeneous mixture thanks to the hydrogen split that is induced immediately downstream of the spray cap. Compared to results shown in Fig. 4b, which have been obtained by adopting the same spray cap and the same SOI, a higher Φ_{Rel} is achieved, since simulations were carried out using a different set of boundary conditions. Even if this change could partially affect the robustness of the analysis, it is however useful to stress once again the large impact that small differences in the cylinder dynamics induced by the variation of the intake pressure and the valve lift profile have on the air-hydrogen mixing process. *Spray Cap v2* results in the lowest level of homogeneity, as indicated by the Φ_{Rel} parameter reaching a value of 51%. Indeed, as reported in Fig. 9b - bottom, hydrogen is vertically stratified, with a higher concentration in the neighboring of the piston that reduces moving toward the cylinder head, resulting in an extremely lean region ($\lambda > 5$) around the spark plug. Moreover, even though *Spray Cap v2* induces the strongest tumble motion, its intensity seems not to be strong enough to release some of the hydrogen that is locked by the swirl. As a matter of fact, most of the injected hydrogen is still guided by the swirl, resulting in an almost stoichiometric ($\lambda \leq 1$) strip on the injector side of the combustion chamber (Fig. 9b - Top). A similar mixture is achieved with *Spray Cap v3,* with a higher hydrogen concentration attached to the liner because of the strong swirl. Nonetheless, some of the injected hydrogen is capable of escaping from it and moves toward the center of the combustion chamber, thus increasing mixture uniformity. Even though *Spray Cap v1* leads to the best mixture uniformity, *Spray Cap v3* was selected as the optimal solution. First, the orientation of the nozzle of the cap toward the center of the combustion chamber favors its scavenging. Hence at the end of the compression stroke, a relatively lean mixture ($\lambda > 2.0$) is achieved inside the cap, reducing the risk of abnormal combustion phenomena. Second, differently from what happens with *Spray Cap v2*, the hydrogen jet impinges on the cylinder liner only after the end of the injection, when its speed is significantly lower compared to that achieved during the injection process. This lowers the likelihood of oil dilution and potential concerns associated with the pre-ignition of the mixture caused by oil droplets.

4.3. Effects of swirl chamfers design

From the analysis of the different spray caps, it turned out that swirl is the main responsible for the poor diffusion and mixing of hydrogen in the combustion chamber. To quantify the impact of the swirl on the properties of the mixture, the intensity of the swirl has been modified by acting on the eccentricity of the intake valve seats (i.e. swirl chamfers). Starting from the base cylinder head, featuring a swirl chamfer only on the long port (Fig. 10 - left) that further increases the swirl induced by the helical shape of the intake ports, two additional configurations were tested. At first two counter swirl-chamfers, generating an opposite swirl compared to that induced by the intake ports, were applied on both the intake valve seats (Fig. 10 - center). Then the counter swirl-chamfer was applied only on the long port, while a concentric chamfer was adopted

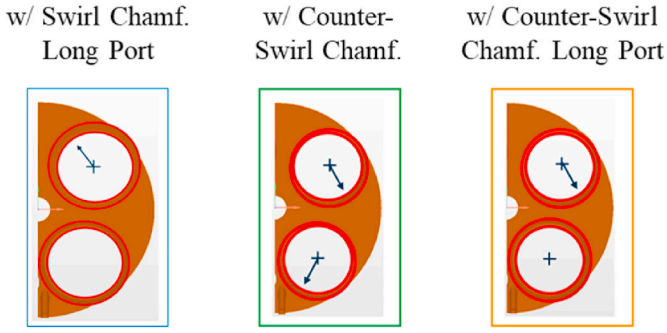

Fig. 10. Intake valve chamfer layouts.

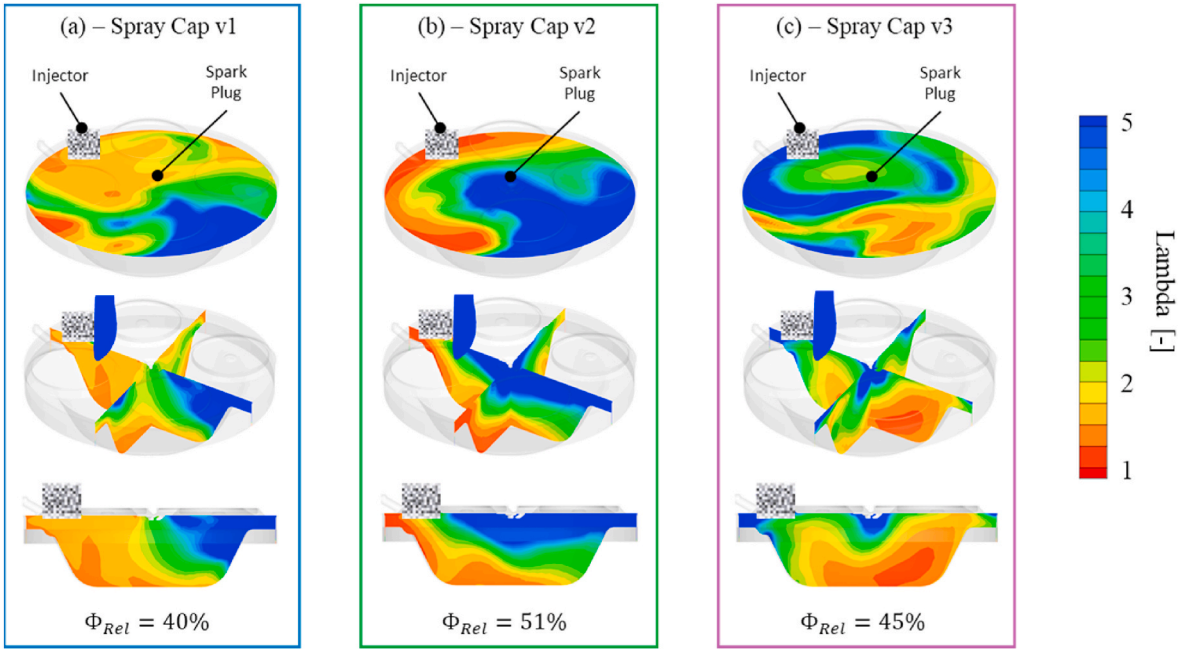

Fig. 9. Lambda distribution 20 CAD before TDC firing for Spray Cap v1 (a), Spray Cap v2 (b), and Spray Cap v3 (c).

on the short port (Fig. 10 - right).

The impact of the intake valve seat eccentricity on the swirl intensity is remarkable. As shown in Fig. 11a, the swirl ratio is positive when adopting the same cylinder head geometry of the original diesel engine (i.e. with the swirl chamfer on the long port). Instead, the swirl ratio becomes negative for the configuration with the counter swirl chamfers on both ports, denoting an opposite swirl rotation direction. On the contrary, a swirl motion with nil intensity is produced by the configuration that features a counter-swirl chamfer only on the long port. The variation of the swirl intensity affects both X-tumble (Fig. 11b) and Y-tumble (Fig. 11c) ratios at the same time. This happens because the hydrogen is deflected by the swirl during the injection, thus modifying its interaction with the combustion chamber walls.

By looking at the lambda distribution 20 CAD bTDCf, a few differences can be highlighted between the two configurations that lead to a quite intense swirl motion (Fig. 12a and b). Indeed, both of them display an asymmetric hydrogen distribution, with a lean pocket on the injector side, a higher fuel concentration located on the opposite side of the combustion chamber, arranged in a half-moon shape, and a vertical

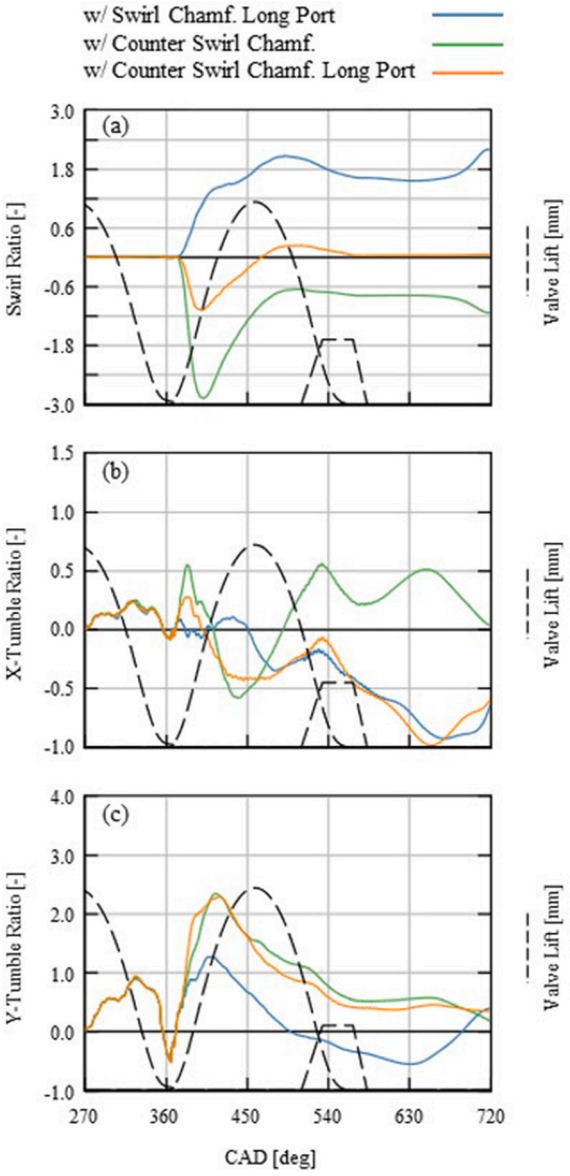

Fig. 11. Swirl Ratio (a), X-Tumble Ratio (b), and Y-Tumble Ratio (c) considering a Swirl Chamfer on the Long Port, Counter Swirl Chamfers on both the Ports and a Counter Swirl Chamfer on the Long Port.

stratification (richer mixture on the piston top and a leaner mixture approaching the spark plug). This similarity is also confirmed by the Φ_{Rel} parameter, that differs by a very small amount between the two cases. The poor homogeneity levels achieved by these two configurations affirm once more the negative influence that swirl intensity has on the proper hydrogen distribution. Instead, a remarkable improvement in terms of mixture homogeneity is obtained with the zero-swirl configuration (Fig. 12c), as confirmed by the sensible Φ_{Rel} reduction. Even though the mixture does not appear as perfectly homogeneous, it is radially stratified, with a $\lambda \sim 2.0$ region close to the spark plug and the $\lambda \sim 3.0$ region close to the liner. This aspect is expected to help in obtaining a more stable flame kernel, reducing cycle-to-cycle variability (CCV). Moreover, a leaner mixture in the peripheral areas of the combustion chamber should reduce losses due to wall heat transfer, increasing thermodynamic efficiency.

All things considered, the configuration with counter swirl chamfers machined only on the long port leads to the best homogeneity level, thanks to the almost nil intensity of the swirl that is generated during the intake process. This aspect is particularly crucial, especially given that most of the current hydrogen engines under development are retrofitted from diesel engines, usually designed to achieve high swirl intensity.

5. Conclusions

In the present work, a 3D-CFD analysis was carried out to analyze and optimize the mixture formation process in a DI-H_2 ICE for off-road applications retrofitted from a diesel engine. To consider the most challenging scenario, simulations were performed in the rated power working point which is characterized by the longest injection duration over the entire engine map and by the shortest time available for hydrogen to spread within the combustion chamber due to the maximum engine revving speed. To avoid the re-design of the entire combustion system, only minor geometrical modifications were considered. More in detail, several injector spray caps were tested to assess their effectiveness in improving mixture homogeneity. Then, a sensitivity analysis on the eccentricity of the intake valve seats was performed to evaluate the impact of the swirl intensity on hydrogen distribution. These analyses were carried out considering the optimal injection phasing resulted from a preliminary sweep of the start of injection (SOI), that was performed to find the best compromise between mixture uniformity and reduction of volumetric efficiency.

The main outcomes can be summarized as follows:

- The SOI advance from 180 CAD to 210 CAD led to a significant improvement in terms of mixture homogeneity thanks to the longest time available for hydrogen to evenly spread within the combustion chamber. Nonetheless, a further SOI advance did not help in increasing hydrogen distribution in the face of sensible filling losses and hydrogen backflow. This happens because in DI H_2-ICE, the injection process influences the evolution of in-cylinder dynamics thanks to the interaction between the high-speed hydrogen jet and the boundaries of the combustion chamber.
- Injector spray caps proved to be a valuable solution for providing a preferential direction to the injected hydrogen. Therefore, the spray cap can be exploited to target specific portions of the combustion chamber, resulting in an additional degree of freedom for the achievement of a mixture with suitable properties. Even if different mixture homogeneity levels were achieved by adopting distinct spray caps, the high intensity of the swirl severely hindered the fast and balanced spread of hydrogen into the cylinder.
- The high swirl intensity induced by the helical shape of the intake ports, adopted without any modifications from the actual diesel engine, can be altered by acting on the eccentricity of the intake valve seats (i.e. swirl chamfers). Specifically, the machining of counter-swirl chamfers on both the intake valves led to an opposite swirl motion pattern, whereas swirl intensity became nil when using a

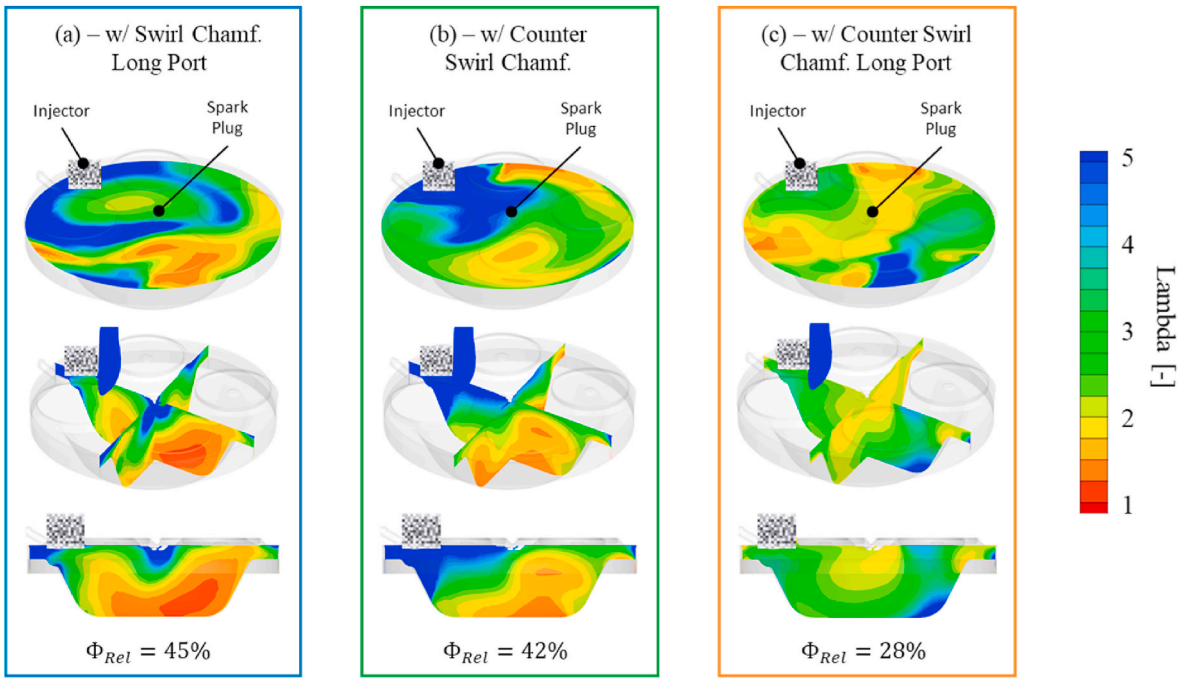

Fig. 12. Lambda distribution 20 CAD before TDC firing considering a Swirl Chamfer on the Long Port (a), Counter Swirl Chamfers on both the Ports (b), and a Counter Swirl Chamfer on the Long Port (c).

counter-swirl chamfer only on the long port. The no-swirl configuration led to the best mixture homogeneity. This evidence suggests that swirl motion has to be carefully considered during the engine design process since it plays a fundamental role in determining the properties of the mixture.

Overall, the relative equivalence ratio was reduced from 50% to 28% operating on the above-mentioned parameters. The sensible improvement of the mixture properties is expected to positively impact both NOx emissions and the risk of abnormal combustion phenomena. Finally, this analysis can pave the way to further research activities concerning the impact of mixture properties on combustion characteristics and pollutant emissions, as well as the possible improvements that could result from a deeper conversion of the overall combustion system.

Declaration of competing interest

The authors declare that they have no known competing financial interests or personal relationships that could have appeared to influence the work reported in this paper.

CRediT authorship contribution statement

A. Scalambro: Writing – original draft, Visualization, Software, Investigation, Formal analysis. **A. Piano:** Writing – review & editing, Methodology. **F. Millo:** Writing – review & editing, Supervision, Project administration, Funding acquisition. **N. Scinicariello:** Writing – review & editing, Supervision, Project administration, Funding acquisition, Conceptualization. **W. Lodi:** Writing – review & editing, Project administration, Conceptualization. **A. Dhongde:** Supervision, Methodology, Conceptualization. **G. Sammito:** Writing – review & editing, Software, Investigation, Formal analysis.

References

[1] https://climate.nasa.gov/.
[2] Sixth assessment report (AR6) of the intergovernmental panel on climate change (IPCC).
[3] IEA - Energy Statistics Data Browser, https://www.iea.org/data-and-statistics.
[4] Masson-Delmotte V, Zhai P, Pörtner HO, Roberts D, et al. Global warming of 1.5° C: IPCC special report on impacts of global warming of 1.5° C above pre-industrial levels in context of strengthening response to climate change, sustainable development, and efforts to eradicate poverty. Cambridge University Press; 2022. https://doi.org/10.1017/9781009157940.
[5] European Commission. Fit for 55': delivering the EU's 2030 climate target on the way to climate neutrality. 2021.
[6] European Commission. The European green deal. 2019. Brussels.
[7] Sens M, Danzer C, Von Essen C, Brauer M, et al. Hydrogen powertrains in competition to fossil fuel based internal combustion engines and battery electric powertrains. In: 42nd international Vienna motor symposium; 2021.
[8] Shadidi B, Najafi G, Yusaf T. A review of hydrogen as a fuel in internal combustion engines. Energies 2021;14(19):6209. https://doi.org/10.3390/en14196209.
[9] Karim GA. Hydrogen as a spark ignition engine fuel. Int J Hydrogen Energy 2003; 28:569–77. https://doi.org/10.1016/S0360-3199(02)00150-7.
[10] Verhelst S, Wallner T. Hydrogen-fueled internal combustion engines. Prog Energy Combust Sci 2009;35(6):490–527. https://doi.org/10.1016/j.pecs.2009.08.001.
[11] Ilbas M, Crayford AP, Yilmaz I, Bowen PJ, et al. Laminar-burning velocities of hydrogen-air and hydrogen-methane-air mixtures: an experimental study. Int J Hydrogen Energy 2006;31(12):1768–79. https://doi.org/10.1016/j.ijhydene.2005.12.007.
[12] Milton BE, Keck JC. Laminar burning velocities in stoichiometric hydrogen and hydrogen-hydrocarbon gas mixtures. Combust Flame 1984;58(1):13–22. https://doi.org/10.1016/0010-2180(84)90074-9.
[13] Das LM. Hydrogen-Oxigen Reaction Mechanism and its implication to hydrogen engine combustion. Int J Hydrogen Energy 1996;21(8):703–15. https://doi.org/10.1016/0360-3199(95)00138-7.
[14] White CM, Steeper RR, Lutz AE. The hydrogen-fueled internal combustion engine: a technical review. Int J Hydrogen Energy 2006;31(10):1292–305. https://doi.org/10.1016/j.ijhydene.2005.12.001.
[15] Verhelst S, Maesschalck P, Rombaut N, Sierens R. Increasing the power output of hydrogen internal combustion engines by means of supercharging and exhaust gas recirculation. Int J Hydrogen Energy 2009;34(10):4406–12. https://doi.org/10.1016/j.ijhydene.2009.03.037.
[16] Wallner T, Nande A, Naber J. Evaluation of injector location and nozzle design in a direct-injection hydrogen research engine. SAE Technical Paper 2008-01-1785 2008. https://doi.org/10.4271/2008-01-1785.
[17] Grabner P, Schneider M, Gschiel K. Formation mechanisms and characterization of abnormal combustion phenomena of hydrogen engines. SAE Technical Paper 2023-32-0168 2023. https://doi.org/10.4271/2023-32-0168.
[18] Thawko A, Tartakovsky L. The mechanism of particle formation in non-premixed hydrogen combustion in a direct-injection internal combustion engine. Fuel 2022; 327:125187. https://doi.org/10.1016/j.fuel.2022.125187.
[19] Thawko A, Eyal A, Tartakovsky L. Experimental comparison of performance and emissions of a direct-injection engine fed with alternative gaseous fuels. Energy Convers Manag 2022;251:114988. https://doi.org/10.1016/j.enconman.2021.114988.

[20] Dober G, Hoffmann G, Piock Borgwarner W, Doradoux L, et al. Application of H2 ICE technology on commercial vehicles. 2022. ISBN 9783000725241.
[21] Das LM. "Hydrogen-fueled internal combustion engines," compendium of hydrogen energy: hydrogen energy conversion, vol. 3. Elsevier; 2015. p. 177–217. https://doi.org/10.1016/B978-1-78242-363-8.00007-4.
[22] Mohammadi A, Shioji M, Nakai Y, Ishikura W, et al. Performance and combustion characteristics of a direct injection SI hydrogen engine. Int J Hydrogen Energy 2007;32(2):296–304. https://doi.org/10.1016/j.ijhydene.2006.06.005.
[23] Dober G, Hoffmann G, Piock WF, Doradoux L, et al. An efficient path to zero CO2 powertrains – BorgWarner's hydrogen injection systems. In: Proceedings of the 43rd international Vienna motor symposium 27 - 29 april; 2022. ISBN 9783950496918.
[24] Li Y, Gao W, Zhang P, Ye Y, et al. Effects study of injection strategies on hydrogen-air formation and performance of hydrogen direct injection internal combustion engine. Int J Hydrogen Energy 2019;44(47):26000–11. https://doi.org/10.1016/j.ijhydene.2019.08.055.
[25] Hamzehloo A, Aleiferis P. Numerical modelling of mixture formation and combustion in DISI hydrogen engines with various injection strategies. SAE Technical Paper 2014-01-2577 2014. https://doi.org/10.4271/2014-01-2577.
[26] Gammaidoni T, Miliozzi A, Zembi J, Battistoni M. Hydrogen mixing and combustion in an SI internal combustion engine: CFD evaluation of premixed and DI strategies. Case Stud Therm Eng 2024. https://doi.org/10.1016/j.csite.2024.104072.
[27] Durand T, Adomeit P, Blomberg M, Jeihouni Y, et al. Combustion chamber development to maximize the performance of the hydrogen combustion engine for the T1 ultimate category of the dakar rally competition. SAE Technical Papers, SAE International 2023. https://doi.org/10.4271/2023-01-0737.
[28] Millo F, Piano A, Rolando L, Accurso F, et al. Synergetic application of zero-, one-, and three-dimensional computational fluid dynamics approaches for hydrogen-fuelled spark ignition engine simulation. SAE Int J Engines 2021;15(4). https://doi.org/10.4271/03-15-04-0030.
[29] Zhang C, Zhao X, Sacchi R, You F. Trade-off between critical metal requirement and transportation decarbonization in automotive electrification. Nat Commun 2023;14(1). https://doi.org/10.1038/s41467-023-37373-4.
[30] Scarcelli R, Wallner T, Matthias N, Salazar V, et al. Numerical and optical evolution of gaseous jets in direct injection hydrogen engines. SAE 2011 world congress and exhibition. 2011. https://doi.org/10.4271/2011-01-0675.
[31] Scarcelli R, Wallner T, Salazar V, et al. Modeling and experiments on mixture formation in a hydrogen direct-injection research engine. SAE Int. J. Engines 2010;2(2):530–41. https://doi.org/10.4271/2009-24-0083.
[32] Addepalli SK, Pei Y, Zhang Y, Scarcelli R. Multi-dimensional modeling of mixture preparation in a direct injection engine fueled with gaseous hydrogen. Int J Hydrogen Energy 2022;47(67):29085–101. https://doi.org/10.1016/j.ijhydene.2022.06.182.
[33] Yosri MR, Palulli R, Talei M, Mortimer J, et al. Numerical investigation of a large bore, direct injection, spark ignition, hydrogen-fuelled engine. Int J Hydrogen Energy 2023;48(46):17689–702. https://doi.org/10.1016/j.ijhydene.2023.01.228.
[34] O'Rourke P, Amsden A. A particle numerical model for wall film dynamics in port-injected engines. SAE Technical Paper 1996:961961. https://doi.org/10.4271/961961.
[35] Ferreira JM, Tinchon A, Coratella C, Oung R, et al. A validation methodology for the 3D-CFD model of a hydrogen injector. In: International stuttgart symposium. Wiesbaden: Springer Fachmedien Wiesbaden; 2023. p. 351–67.
[36] Rouleau L, Duffour F, Walter B, Kumar R, et al. Experimental and numerical investigation on hydrogen internal combustion engine. SAE Technical Paper 2021-24-0060 2021. https://doi.org/10.4271/2021-24-0060.
[37] Aljabri H, Silva M, Houidi MB, Liu X, et al. Comparative study of spark-ignited and pre-chamber hydrogen-fueled engine: a computational approach. Energies 2022;15(23):8951. https://doi.org/10.3390/en15238951.
[38] Babayev R, Andersson A, Dalmau AS, Im HG, et al. Computational characterization of hydrogen direct injection and nonpremixed combustion in a compression-ignition engine. Int J Hydrogen Energy 2021;46(35):18678–96. https://doi.org/10.1016/j.ijhydene.2021.02.223.
[39] Dhongde A, Recker P, Sankhla H, et al. Advanced simulation methodologies for hydrogen combustion engines. ATZ Heavy Duty worldwide 2021;14:46–51. https://doi.org/10.1007/s41321-021-0456-9.